HHS Public Access

Author manuscript

Mater Horiz. Author manuscript; available in PMC 2021 November 01.

Published in final edited form as:

Mater Horiz. 2020 November 1; 7(11): 3028–3033. doi:10.1039/d0mh00755b.

Augmenting T-cell responses to tumors by *in situ* nanomanufacturing

Mohammad Mahdi Hasani-Sadrabadi[a], **Fatemeh S. Majedi**[a], **Matthew L. Miller**[b], **Timothy J. Thauland**[c], **Louis-S. Bouchard**[a,d], **Song Li**[*,a], **Manish J. Butte**[*,b,c,e]

[a]Department of Bioengineering, University of California Los Angeles, Los Angeles, CA, 90095 USA

[b]Molecular Biology Institute, University of California Los Angeles, Los Angeles, CA, 90095 USA

[c]Department of Pediatrics, Division of Immunology, Allergy, and Rheumatology, University of California Los Angeles, Los Angeles, CA, 90095 USA

[d]Department of Chemistry and Biochemistry, University of California Los Angeles, Los Angeles, CA, 90095 USA

[e]Department of Microbiology, Immunology, and Molecular Genetics, University of California Los Angeles, Los Angeles, CA, 90095 USA

Abstract

Recent innovations in immunoregulatory treatments have demonstrated both the impressive potential and vital role of T cells in fighting cancer. These treatments come at a cost, with systemic side effects including life-threatening autoimmunity and immune dysregulation the norm. Here, we developed an approach to locally synthesize immune therapies and in this way, avoid systemic toxicity. Rather than just encapsulating cytokines, we endowed our nanoparticles with transcriptional and translational machinery to *make* cytokines locally, *in situ*, and on demand (activated by light). We demonstrated the capabilities of these particles *in vitro* and *in vivo*, in a mouse model of melanoma, and showed that tumor-infiltrating T cells were more highly activated in the context of these “microfactory” particles that make the synthetic cytokine.

Introduction

Cytokine therapy, checkpoint inhibitor therapy, and other forms of immunomodulation have proven exceptionally potent in the fight against cancer. However, globally altering the immune system can lead to adverse systemic effects, including severe inflammation, autoimmunity, and increased susceptibility to infection[1,2]. Ideally, immunomodulatory factors would be provided at the site of the tumor – where they are needed, and allowing for

[*]Corresponding authors: songli@ucla.edu (SL) and mbutte@ucla.edu (MJB).

Conflicts of interest

There are no conflicts to declare.

Supporting Information is available from the Wiley Online Library or from the author.

Electronic Supplementary Information (ESI) available: [details of any supplementary information available should be included here]. See DOI: 10.1039/x0xx00000x

higher concentrations - while avoiding systemic exposure. Moreover, other diseases also may arise if there is a physiological inability to make enough key protective factors when most needed. Nano-bio-manufacturing affords the opportunity to synthesize specific factors *in situ* and deliver to cells while employing controls on timing and spatial delivery that cannot be achieved by biological systems.

The *in situ* biosynthesis of proteins allows for a number of features not attainable by other approaches to deliver proteins exogenously: tunable initiation to eliminate the systemic toxicity of basal/continuous expression and controlled release to locally focus the site of the cytokines' activity. Here we propose a new approach in which we implemented the *in situ* synthesis of the interleukin 2 (IL-2) at the site of immunological action to tune T cell fate locally and to safely augments the immune response to promote clearance of cancer.

Results and Discussion

Our approach is predicated on the nanoencapsulation of cell-free transcription and translation machinery, coupled with a mechanism to control protein production (Figure 1a). Here we first encapsulated cell-free protein biosynthesis systems (also known as *in vitro* transcription-translation kits) into liposomes to contain the reagents. It has been reported that liposomal encapsulation can achieve transcription and translation of functional proteins and enzymes[3]. Here we used our microfluidics approach to prepare nanoliposomes[4]. A broad size range of nanoliposomes (50–400 nm) and narrow polydispersity was achieved by adjusting relative microfluidic flow rates (Figure 1b,c).

To test how the size of liposomes affected their ability to hold DNA cargo, we encapsulated three sizes of plasmids (3300 – 6500 bp) within six sizes of nanoliposomes (40–400 nm) and measured encapsulation. The efficiency of loading depended on the sizes of both the cargo and the nanoliposomes (Figure 1d). In contrast to microfluidic approaches, formation of nanoliposomes by conventional bulk mixing and extrusion techniques with porous membranes produced polydisperse particles of 100–800 nm diameter (Figure 1c), and thus could incur variable inefficiencies in loading plasmids. Based on these data, nanoliposomes of 350 nm diameter ("uF-4") were able to encapsulate substantial amount of all three plasmids and were with selected for further investigation.

Our first goal was to demonstrate temporal control over protein production in the nanofactories. We tested whether a UV-caged ATP (DMNPE-caged ATP) could efficiently control protein synthesis[5]. Exposure to UV uncages ATP and should initiate transcription and translation. We started by encapsulating transcription/translation machinery provided by cellular extracts, an IL2-GFP plasmid (AddGene #67053), and caged ATP into nanofactories. Imaging of nanofactories revealed no detectable basal expression of GFP, while UV exposure at 360–480 nm wavelength for 10 s (at 80 mW/cm^2; pH 7.4; 37 °C) uncaged the ATP and resulted in robust GFP expression in 30 min (Figure 1e). As GFP only fluoresces if IL-2 and GFP are folded properly, these observations show the fabricated nanoparticles contained all components necessary for transcription, translation, and folding of cytokines on demand. Nanofactories >100 nm in size were capable of producing GFP, and larger nanofactories were more productive (Figure 1f). Improved encapsulation efficiency of

protein production machineries into microfluidic assisted synthesized liposomes resulted in protein synthesis with higher efficiency.

In order to localized synthesis and controlled delivery of cytokine at tissue level, we fabricate artificial cells that not only mimic the size, shape, and mechanics of lymphocytes like T cells [6], but also contain the synthetic machinery for transcription and translation of functional cytokine, and elements that allow for precisely controlled activation and release of the cytokine. To load the liposomal nanofactories into delivery vehicles with additional capabilities, we microfluidically encapsulated them into alginate-based microparticles (Figure 2a), with an average of 443 nanoliposomes per microparticle (Supplemental Figure 1). To facilitate magnetic purification of the "microfactories," we embedded superparamagnetic iron oxide nanoparticles (SPIONs) during microfluidic synthesis as we reported before [3]. Microparticle factories showed no basal expression of IL2-GFP. Upon UV-illumination, protein synthesis from the microparticle factories plateaued at ~60 min (Figure 2b–c).

To demonstrate the capability of these microfactories to be delivered and activated *in vivo*, we "tattooed" mouse skin with IL2-GFP microfactories and exposed part of the tattooed skin to UV light. These wavelengths of light allow for ~1 mm of penetration in the epidermis[7]. Within 60 min after UV exposure, GFP production was evident only in the UV-exposed area (Figure 2d). This result confirmed that microfactories can survive *in vivo* and can produce functional protein after UV activation.

Next, we examined the efficiency of nanoliposome-produced IL-2 in augmenting T cell activation. IL-2 has been FDA-approved for treatment of several cancers since the 1980s[8], but clinical use has been limited due to severe side effects, some of which include vascular leak syndrome, hypotension, and cardiac toxicity[9]. Other groups have engineered approaches to mitigate the toxicity of IL-2[9,10]. For the rest of our studies, we employed a synthetic IL-2 (Super2) (Supplemental Figure 2), which has the advantage of activating T cells expressing the receptor most commonly found on naïve T cells – comprising IL2Rβ (CD122) and IL2Rγ (CD132) – but not requiring the high affinity IL2Rα chain (CD25) that is found on activated and regulatory T cells[11].

We co-cultured naïve T cells with Super2-producing nanofactories either as free particles, or encapsulated in alginate microfactories. For some particles, alginate was conjugated with heparin[12] before encapsulation to test whether heparin could prolong release of the cytokine. For others, the microfactories were coated with the phosphatidylcholine lipid POPC for a similar test. We showed that the duration of Super2 release increased over 10-fold by heparin incorporation and lipid encapsulation, with 50% release extended from 5.4 h to 62 h (Figure 3a). To assess the impact on T cells, we measured *in vitro* proliferation and found that free nanofactories (fastest cytokine release) elicited the highest expansion early (day 4), but heparin-lipid encapsulation of nanofactories (slowest cytokine release) resulted in the greatest sustained expansion ($p < 0.005$ compared to each other condition) (Figure 3b). To study the mechanism underlying enhanced proliferation, we found that enhanced viability (Figure 3c, Supplemental Figure 3), expression of Granzyme B (Figure 3d, Supplemental Figure 4), and IFN-γ secretion (Figure 3e, Supplemental Figure 5) correlated with enhanced

proliferation. Sustained release of synthetic IL-2 resulted in a potent effector pool but modest upregulation of CD25 and minimal downregulation of CD62L (Figure 3f, Supplemental Figure 6). In contrast, exposure to rapidly synthesized Super2 by free nanofactories promoted downregulation of CD62L and upregulation of CD25, consistent with prior reports[13,14]. Thus, sustained protein synthesis and exposure to Super2 generated a differentiation state of effector T cells with strong killing potential.

To test whether accentuation of T cell activation by our microfactories could also augment antigen-specific killing of cancer cells, we cultured naïve OT-I T cells with Super2 microfactories for 3 days, then added fluorescently-labeled B16-ova melanoma cells as targets. T cells co-cultured with microfactories showed enhanced killing as compared to soluble IL-2 (Figure 3f,g, Supplemental Figure 7). Taken together, these results demonstrate that T-cell activation, proliferation, and killing were enhanced by Super2 synthesis from microfactories.

To test the impact of microfactories on T-cell function *in vivo*, we subcutaneously injected mice with B16-ova melanoma cells on both flanks (Figure 4a). After the tumors became palpable, Super2 microfactories were injected subcutaneously into the same regions as the tumors, and activated OT-I T cells were transferred intravenously. As a control, some mice received OT-I T-cells plus microfactories producing only GFP. As another control, some mice received no T cells and no microfactories but rather only saline injections (“PBS”). Even though both flanks received Super2 microfactories, we illuminated only one flank with UV light (“treated” side), the other side was covered from UV light (“untreated” side) as a control. As a control for the potential treatment effect that a short burst of UV could provide, as a control some mice with tumor and OT-I T cells received no microfactories and instead were treated with an identical exposure of UV light. As another control for the effect of IL-2, intratumoral injection of soluble IL-2 was given to some mice. The UV “treated” side showed virtually no growth of the tumor (Figure 4b,c, Supplemental Figure 8), whereas the unilluminated side (UV-“untreated”) showed substantial growth, comparable to mice that received OT-I T cells and local IL-2 (Figure 4b,c), comparable to the mice that received OT-I T cells and GFP microfactories, and comparable to the mice that received OT-I T cells and only local UV exposure (Supplemental Figure 8). Thus, Super2 microfactories dramatically enhanced local tumor clearance by the transferred antigen-specific T cells. Because the particles here were injected intratumorally, the UV “on switch” was not strictly necessary for treatment purposes, but allowed us here to make a legitimate comparison with the contralateral side of the mice, which received “full” microparticles but did not receive UV irradiation.

We then investigated the mechanism of the enhanced tumor clearance and found that illuminated (“treated”) Super2 microfactories elicited greater expansion of tumor-infiltrating cytotoxic T cells compared to the unilluminated side (“untreated”) or controls (Figure 4d), raising the ratio of cytotoxic effectors to helper T cells substantially (Figure 4e). There was also a disproportionate enrichment of antigen-specific OT-I T cells on the illuminated side (Figure 4f). We found that Super2 microfactories drove higher expression of cytotoxin granzyme B in T cells (Figure 4g; Supplemental Figure 9a). Exposure to Super2 also enhanced co-expression of CD44 with Granzyme B, especially among OT-I T cells

(Supplemental Figure 9b–c). Together, these results provide a mechanistic explanation for the enhanced clearance of tumors by illuminated Super2 microfactories. We examined the T-cell exhaustion marker PD-1 on intratumoral T cells and found comparable levels across treatments, supporting the well-established notion that fast-growing tumors like B16 melanoma do not rely on PD-1-based T cell exhaustion solely for immune evasion[15–17] (Supplemental Figure 9d–e).

Conclusions

Our approach embodies a technological foundation for on-demand production and release of therapeutic proteins at the site of immunological action to safely augment the immune response to solid tumors. Similar approaches have demonstrated luciferase production from nanoparticles[3] and even anti-tumor enterotoxins[18]. Moving towards human translation with this approach would probably see abandonment of UV activation, especially if the particles are injected in the peri- or intra-tumoral area. This platform can also enable control over sequential production of multiple factors during the therapeutic course, which is not trivial with competitive technologies.

This platform affords the opportunity to synthesize specific factors *in situ* while employing controls on timing and spatial delivery that are difficult to achieve in traditional cancer therapies.

Supplementary Material

Refer to Web version on PubMed Central for supplementary material.

Acknowledgments

Interlukin-2 used for this study was provided by the BRB Preclinical Repository of the National Cancer Institute, Frederick, MD, USA. We acknowledge support from the NIH (R01 GM110482 to MJB and 1R56DE029157 to SL).

Notes and references

1. Dhodapkar KM, Curr. Opin. Immunol, 2019, 61, 54–59. [PubMed: 31557690]
2. Waldmann TA, Cold Spring Harb. Perspect. Biol,, DOI:10.1101/cshperspect.a028472.
3. Schroeder A, Goldberg MS, Kastrup C, Wang Y, Jiang S, Joseph BJ, Levins CG, Kannan ST, Langer R and Anderson DG, Nano Lett, 2012, 12, 2685–2689. [PubMed: 22432731]
4. Hasani-Sadrabadi MM, Taranejoo S, Dashtimoghadam E, Bahlakeh G, Majedi FS, Vandersarl JJ, Janmaleki M, Sharifi F, Bertsch A, Hourigan K, Tayebi L, Renaud P and Jacob KI, Adv. Mater, 2016, 28, 4134–4141. [PubMed: 27001745]
5. Monroe WT, McQuain MM, Chang MS, Alexander JS and Haselton FR, J. Biol. Chem, 1999, 274, 20895–20900. [PubMed: 10409633]
6. Hasani-Sadrabadi MM, Majedi FS, Bensinger SJ, Wu BM, Bouchard L, Weiss PS and Moshaverinia A, Adv. Mater, 2018, 30, 1706780.
7. Meinhardt M, Krebs R, Anders A, Heinrich U and Tronnier H, J. Biomed. Opt, 2008, 13, 044030. [PubMed: 19021357]
8. Lotze MT, Matory YL, Rayner AA, Ettinghausen SE, Vetto JT, Seipp CA and Rosenberg SA, Cancer, 1986, 58, 2764–2772. [PubMed: 3490903]
9. Jiang T, Zhou C and Ren S, Oncoimmunology, 2016, 5, 1–10.

10. Zhang Y, Li N, Suh H and Irvine DJ, Nat. Commun, 2018, 9, 6. [PubMed: 29295974]
11. Levin AM, Bates DL, Ring AM, Krieg C, Lin JT, Su L, Moraga I, Raeber ME, Bowman GR, Novick P, Pande VS, Fathman CG, Boyman O and Garcia KC, Nature, 2012, 484, 529–533. [PubMed: 22446627]
12. Majedi FS, Hasani-Sadrabadi MM, Kidani Y, Thauland TJ, Moshaverinia A, Butte MJ, Bensinger SJ and Bouchard L-S, Adv. Mater, 2018, 30, 1703178.
13. Manjunath N, Shankar P, Wan J, Weninger W, Crowley MA, Hieshima K, Springer TA, Fan X, Shen H, Lieberman J and Von Andrian UH, J. Clin. Invest, 2001, 108, 871–878. [PubMed: 11560956]
14. Obar JJ and Lefrançois L, J. Immunol, 2010, 185, 263–272. [PubMed: 20519649]
15. Juneja VR, McGuire KA, Manguso RT, LaFleur MW, Collins N, Haining WN, Freeman GJ and Sharpe AH, J. Exp. Med, 2017, 214, 895–904. [PubMed: 28302645]
16. Chen S, Lee LF, Fisher TS, Jessen B, Elliott M, Evering W, Logronio K, Tu GH, Tsaparikos K, Li X, Wang H, Ying C, Xiong M, Van Arsdale T and Lin JC, Cancer Immunol. Res, 2015, 3, 149–160. [PubMed: 25387892]
17. Kleffel S, Posch C, Barthel SR, Mueller H, Schlapbach C, Guenova E, Elco CP, Lee N, Juneja VR, Zhan Q, Lian CG, Thomi R, Hoetzenecker W, Cozzio A, Dummer R, Mihm MC, Flaherty KT, Frank MH, Murphy GF, Sharpe AH, Kupper TS and Schatton T, Cell, 2015, 162, 1242–1256. [PubMed: 26359984]
18. Krinsky N, Kaduri M, Zinger A, Shainsky-Roitman J, Goldfeder M, Benhar I, Hershkovitz D and Schroeder A, Adv. Healthc. Mater, 2018, 7, 1–10.

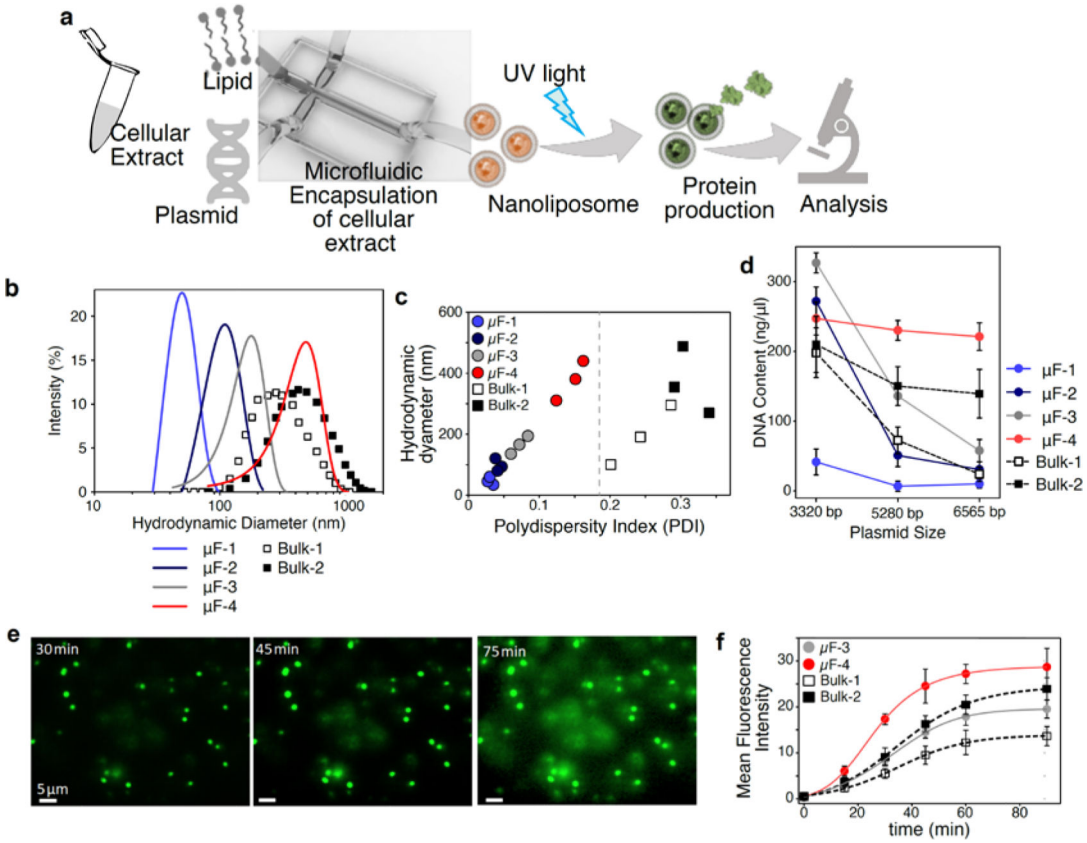

Figure 1. Characterization of nanofactories *in vitro.*

a, Microfluidic system used to make monodisperse, synthesis-capable nanoliposomes. **b**, Dynamic light scattering (DLS) was used to analyze size of nanoliposomes fabricated by microfluidic flows or bulk synthesis. **c**, Polydispersity of microfluidically synthesized particles is much smaller (more uniform) than those synthesized by bulk process. **d,** Efficiency of encapsulation of DNA of different sizes as a function of nanoparticle diameter. **e**, Fluorescent images of IL2-GFP producing nanoliposomes at 30, 45, and 75 min after UV illumination. Scale bar: 5 μm. **f**, Kinetics of IL2-GFP expression inside nanoliposomes of different sizes after triggering of caged-ATP by UV. Mean +/− SD is shown, n=10.

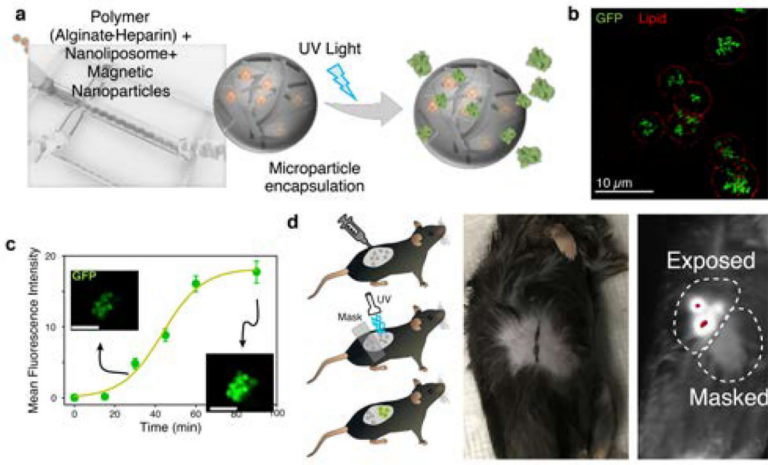

Figure 2. Characterization of microfactories.

a, Microfluidic generation of alginate-heparin microfactories encapsulating protein producing nanoliposomes (artificial cells). These microfactories were subsequently coated with lipid bilayers. **b**, Fluorescent image of GFP production in alginate-heparin microfactories 90 min after UV exposure. Lipid membrane around microfactories stained using DiD fluorescent lipophilic cationic indocarbocyanine dye. **c**, Kinetics of GFP expression inside alginate-heparin microfactories. Mean +/− SD is shown, n=10. **d**, Fluorescence of IL-2-GFP “tattoo” in UV-illuminated region, showing that IL-2 synthesis is local.

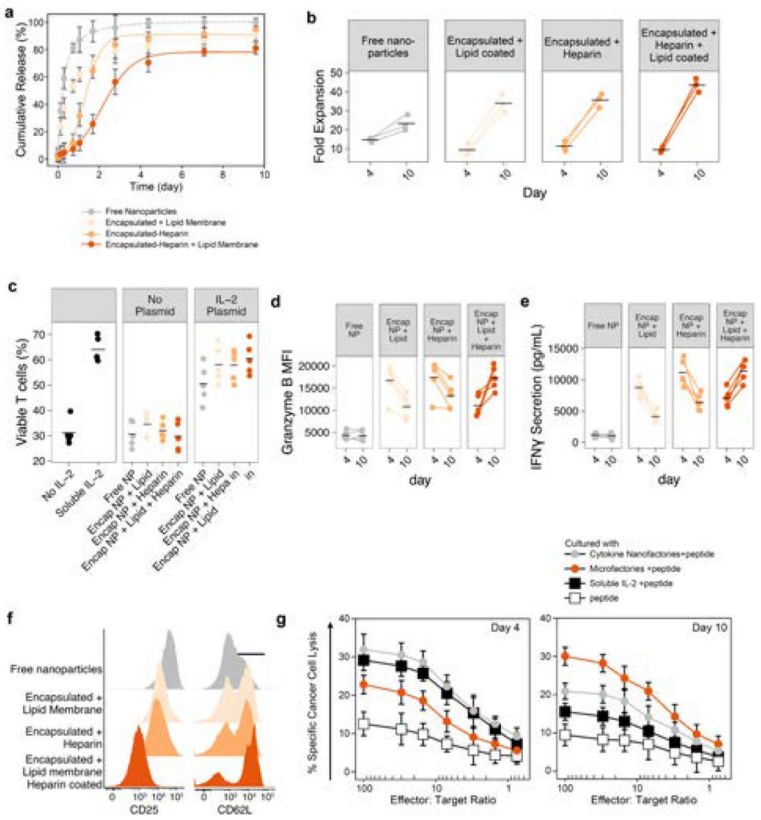

Figure 3. *In vitro* activity of Nano- and micro-factores.

a, Release of Super2 from free nanoliposomes as compared to nanoparticles encapsulated within alginate microparticles that are further endowed with a lipid coat or heparin or both after UV triggering of production. **b**, Expansion of pre-activated primary mouse T cells cultured in the presence of the indicated synthesis platforms. n=3 independent replicates. Mean shown. **c**, T cell viability after co-culture with nanofactories or encapsulated nanofactories. **d-e**, Activation and differentiation markers on day 4 and 10 of co-culture including granzyme B (**d**), IFN-γ (**e**). **f**, Activation markers on day 10 of co-culture with T cells, data representative of 3 independent experiments. **g**, Chromium (^{51}Cr) release assays shows antigen peptide-specific and cytotoxicity of TCR transgenic CD8+ T cells after 4 or 10 days of co-culture with particles as listed. Cytotoxic activity was examined at different ratios of 100:1, 30:1, 15:1, 7:1, 3:1, 1.5:1, and 0.75:1 of treated T cells to tumor cells. The data are presented as Mean ± SD of 3 independent experiments.

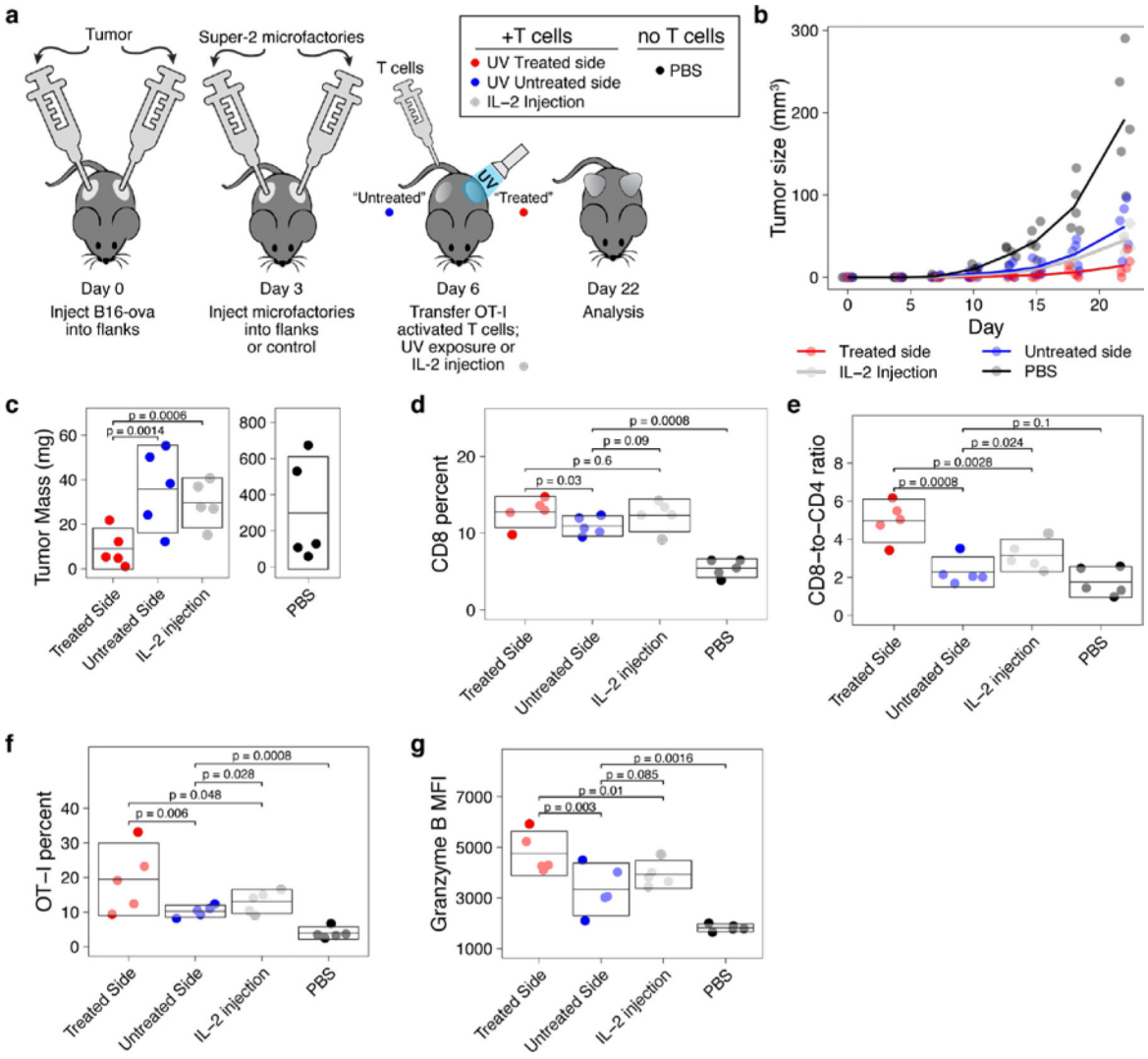

Figure 4. Cytokine microfactories eliminate tumors by enhancing T cell activation.

a, Experimental protocol. **b**, Tumor growth over time. **c**, Tumor mass at day 22, note separate vertical axes. On day 22 in tumor T cells: **d**, CD8 T cells; **e**, CD8-to-CD4 ratio; **f**, Preferential expansion of transferred, antigen-specific T cells; and **g**, Mean fluorescence intensity of granzyme B expression. Each dot is a mouse, box is permuted mean and 95% CI. All p-values have been adjusted for multiple comparisons.